Photoinitiated Synthesis of Mixed Polymer Brushes of Polystyrene and Poly(methyl methacrylate)

Jianxin Feng,[†] Richard T. Haasch,[‡] and Daniel J. Dyer*,[†]

Department of Chemistry, Southern Illinois University, Carbondale, Illinois 62901-4409, and The Frederick Seitz Materials Research Laboratory, University of Illinois, 104 S. Goodwin, MC 230, Urbana, Illinois 61801

Received June 30, 2004; Revised Manuscript Received September 23, 2004

ABSTRACT: We describe the synthesis of mixed, or binary, polymer brushes containing polystyrene (PS) and poly(methyl methacrylate) (PMMA). These films were synthesized by a grafting-from (GF) strategy from gold substrates that were coated with a bis-thiol free radical photoinitiator, similar to 2,2′-azobis-(isobutyronitrile) (AIBN). The PS layer was 70 nm thick for all substrates, and the PMMA was varied up to 700 nm. The number-average molecular weight (M_n) of the ungrafted polymers was determined by gel permeation chromatography (GPC) and multiangle light scattering (MALS); the M_n for bulk PS and PMMA was ∼57 000 and ∼515 000 Da, respectively. The air/liquid interface was probed by static water contact angles (θ) and X-ray photoelectron spectroscopy (XPS). We found that both θ and the oxygen concentration varied depending on whether the substrate was immersed in a nonselective solvent (tetrahydrofuran) or selective solvent for PS (cyclohexane) or PMMA (isobutanol). The morphology was monitored by atomic force microscopy (AFM), and we observed a dimple-type structure in cyclohexane and isobutanol, with less nanophase separation after immersion in tetrahydrofuran. Reflection−absorption infrared spectroscopy (RAIRS) was used to quantify the % PMMA in the binary brushes, which ranged from 0 to 90%, and was confirmed by XPS. These substrates exhibited reversible switching, and both lateral and layered nanophase separation were observed. The elasticity of a mixed brush was probed by AFM and was found to lie between that of neat PS and PMMA.

Introduction

The design and synthesis of polymer thin films that respond to environmental perturbations is an important goal in contemporary polymer science. These so-called "smart" materials can adapt to their environment and alter their interfacial properties to perform various functions. In particular, polymer brushes offer a unique approach to the synthesis of well-defined structures with controlled functionality on the nanometer scale.[1] Polymer brushes consist of polymer chains that are adsorbed or tethered to a substrate or interface. These organic films will impact a variety of fields including biomaterials[2] for tissue engineering,[3] drug delivery,[4,5] implants and cell adhesion,[6] and protein recognition.[7] Other areas include adhesion and wetting,[8] microfluidics,[9] microfabrication,[10−12] molecular recognition,[13] chemical sensing,[14] and organic synthesis.[12,13,15] However, to realize this potential, we require a fundamental understanding of the dynamics of these polymer films and well-defined protocols for their synthesis and characterization.

Inorganic and organic substrates can be modified with organic polymers by a variety of techniques. In particular, "grafting-from" (GF) strategies, or surface-initiated polymerization (SIP), offer distinct advantages over alternative modes of deposition such as spin-casting or the "grafting-to" (GT) approach. For instance, a cast film is merely adsorbed, or physisorbed, to a surface and may deadsorb under various conditions, particularly in organic solvents. Polymers that are grafted to a substrate are more robust and may stretch away from the substrate when the grafting density is sufficiently high. However, the GT technique typically yields low-density polymer brushes because, once grafted, the chains inhibit diffusion of additional reactive polymers to the active functional groups at the surface. In contrast, the GF technique utilizes a polymer initiator that is covalently linked to the surface by a self-assembled monolayer (SAM) so that the polymer grows out away from the substrate and always remains tethered. Where GT films typically exhibit thicknesses of less than 10 nm, GF films may span a broad range from a few nanometers to greater than 1 μm.

Polymer brushes have been synthesized by a variety of initiating mechanisms, and several excellent reviews have been published.[1,16] However, for many applications radical polymerization is preferred due to a tolerance for moisture and a wide variety of organic functional groups. Furthermore, photochemistry is a convenient method for the initiation of free radicals and allows for the lithographic patterning of planar substrates.[17−19] Typical substrates consist of glass microscope slides or silicon wafers that may also be coated with gold. The SAMs are easily prepared from chloro- or alkoxysilane precursors when the substrate is glass or silicon, whereas thiol and disulfide precursors can be used for gold or silver. Photopolymerizations may also be initiated from polymer substrates after plasma treatments[20] or by covalently linking initiators to the preformed polymer.

Recently, polymer brushes that are composed of two different polymers have been described. These so-called "mixed brushes", also referred to as "binary brushes", may exhibit dynamic reorganization when the polymers are soluble in different solvents. For instance, Minko and Stamm have shown that the surface of a mixed brush of polystyrene (PS) and poly(vinylpyridine) (PVP) may be switched from a hydrophobic surface to hydrophilic by immersion into selective solvents such as toluene or aqueous acid.[21] As Figure 1b illustrates, both

[†] Southern Illinois University.
[‡] University of Illinois.
* Corresponding author. E-mail: ddyer@chem.siu.edu.

10.1021/ma048681w CCC: $27.50
Published on Web 11/13/2004

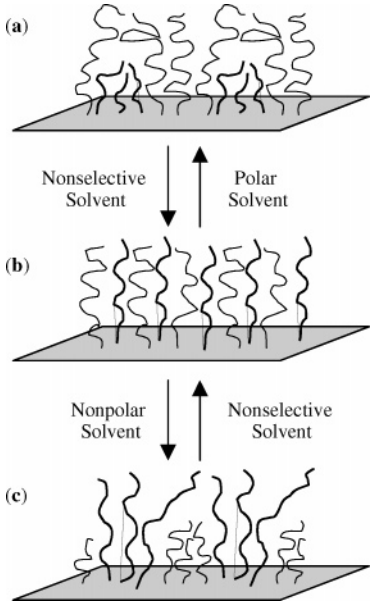

Figure 1. Switching behavior of a mixed brush composed of nonpolar and polar homopolymer chains after immersion into: (a) a polar solvent, which brings the polar polymer to the air/liquid interface while the nonpolar chains aggregate within the interior of the film; (b) a nonselective solvent, where both polymers are soluble and diffuse to the air/liquid interface; and (c) a nonpolar solvent, which brings the nonpolar chains to the air/liquid interface and the polar polymer aggregates within the interior of the film.

polymers are soluble in a nonselective solvent and will diffuse to the liquid interface. However, upon immersion into a polar solvent that is selective for the polar polymer, the nonpolar chains aggregate into the interior of the film, and the polar chains diffuse toward the liquid interface; the reverse holds for a nonpolar solvent that is selective for the nonpolar chains. Mixed brushes have been synthesized by GT and GF techniques and have included a variety of polymers. For instance, a number of studies have focused on polyelectrolyte brushes,[22−24] while others have examined binary systems of PVP with PS,[21,25−27] isoprene,[28] and a PS−indene copolymer.[29] In addition, the groups of Minko and Tsukruk have examined the switching, morphology, and mechanical properties of binary brushes containing poly(pentafluorostyrene) (PPFS) and poly(methyl acrylate) (PMA),[30−32] poly(methyl methacrylate) (PMMA),[33] and PVP.[34]

Little is known about the dynamics of the switching process or the bulk morphology in mixed brushes. Theoretical studies have modeled single-component brushes[35] and binary brushes[33,36] and suggested three phases. In particular, a homogeneous phase exists in binary brushes whereby both components are present at the air or liquid interface; this occurs in a nonselective solvent (Figure 1b). In addition, a "ripple" phase occurs when compatible chains aggregate in a lateral direction (i.e., parallel to the substrate). Furthermore, a layered phase may exist whereby the chains phase-separate into layers perpendicular to the substrate, where the outer layer is compatible with the selective solvent. Minko and co-workers have suggested that lateral and perpendicular phase separation occur simultaneously for mixed brushes of PMMA and PPFS.[33] In this case a nonselective solvent favors a ripple state due to nanophase separation of the two incompatible polymers. Treatment with a selective solvent leads to a "dimple" phase with

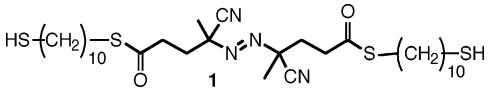

Figure 2. Thiol initiator based on the structure of 2,2′-azobis(isobutyronitrile) (AIBN).

lateral and perpendicular phase separation. The majority of experimental studies to date suggest a combination of lateral and perpendicular segregation, favoring the former.

The work described herein is focused on the synthesis and characterization of binary brushes composed of PS and PMMA from SAMs of 4,4′-azobis[(1,10-dimercaptodecyl)-4-cyanopentanoate] (**1**) on gold (Figure 2). We will compare our results to that of cast films of PS/PMMA[37] as well as Brittain's work on grafted block copolymers,[38,39] Russell's work with grafted random copolymers,[40] and binary brushes of PS/PMMA from Zhao.[41−43] The binary brushes that we have synthesized are much thicker than any reported previously, and they exhibit high grafting densities and very large morphological changes upon immersion into various solvents. Furthermore, we report a complementary approach for confirming the bulk and surface composition of mixed brushes with X-ray photoelectron spectroscopy (XPS) and reflection−absorption infrared spectroscopy (RAIRS).

Experimental Section

Materials. Test grade silicon (100) wafers (p-type, polished on one side) were purchased from waferworld.com. Styrene and methyl methacrylate were purchased from Acros Chemicals; all other solvents and reagents were purchased from Fisher Scientific. Gold was 99.999% pure and purchased from Electron Microscopy Sciences. Styrene was purified by passage through a column filled with Alumina A super 1 (Fisher). Methyl methacrylate was purified by passage through a column filled with inhibitor-remover packing resin (Aldrich), followed by distillation. HPLC grade toluene was distilled. Cyclohexane, tetrahydrofuran (THF), and isobutanol were used as received.

Polymerization. The SAMs of **1** were prepared according to previously published procedures,[44,45] and the monolayer structure was confirmed by RAIRS, ellipsometry, and water contact angle prior to polymerization. Purified styrene (2.5 mL) and the initiator-coated gold substrate were placed in a Schlenk tube. The tube was degassed by using three successive freeze−pump−thaw cycles and then was backfilled with argon. The tube was irradiated for 6 h in a Rayonet photochemical chamber using 300 nm UV light. The photochemical chamber was continuously purged with compressed air to maintain a constant temperature (∼27 °C). The substrate was then removed from the Schlenk tube and rinsed with THF, and the residual physisorbed polymer was removed with a water-cooled jacketed Soxhlet extractor for 5 h. The PS-coated gold slide was then placed into a clean Schlenk tube along with 4 mL of a 50% (w/w) solution of methyl methacrylate in toluene. The same procedure was followed, except the reaction time was varied and the Soxhlet extraction lasted 24 h.

Contact Angle Measurements. Static contact angles were measured with a Tantec contact angle meter (model CAM Micro) at room temperature. Contact angles were averaged from at least three different spots for each substrate.

Thickness Measurements. The thickness of the SAM, polystyrene, and mixed brush films on gold substrates were obtained with a Nanofilm Technologies I-Elli2000 imaging ellipsometer equipped with a 230 mW Nd:YAG laser (532 nm); an incident angle of 70° was used for all measurements. The optical constants n and k (refractive index and the extinction coefficient, respectively) were measured on a bare gold wafer. Refractive indices of 1.46, 1.49, and 1.59 were used for the

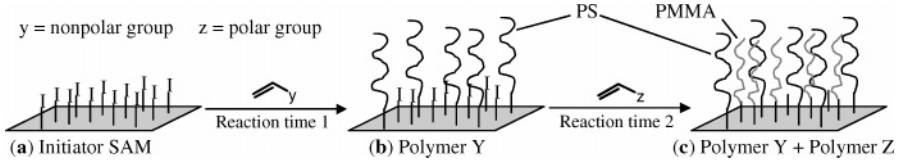

Figure 3. Synthetic strategy for mixed brushes. (a) The initiator self-assembled monolayer is reacted with monomer Y to form a polymer brush. (b) Initiator is still present after the first polymerization, so the reaction may continue with a second monomer Z. (c) A mixed brush is formed with a random distribution of the two polymers.

calculation of the thickness of initiator SAMs, PMMA, and PS films, respectively. A weighted average of refractive indices of PMMA and PS was used for mixed brushes. Data were collected and averaged over at least five measurements.

Reflection−Absorption Infrared Spectroscopy. RAIR spectra were recorded following deposition of the initiator SAM and after the polymerizations. Infrared spectra were recorded on a Nicolet-670 FTIR spectrometer equipped with a liquid nitrogen cooled MCT-B detector and a PIKE grazing angle accessory; all spectra were collected at an 80° grazing angle. The sample chamber was purged with nitrogen gas for 20 min (30 mL/min) prior to data acquisition. Data were averaged over 60 scans at 4 cm^{-1} resolution; an atmospheric suppression algorithm was utilized from the Omnic software. For the concentration studies the difference in extinction coefficients was assumed to be negligible (i.e., $k = 1$).

The calibration curve was obtained from PS and PMMA standards that were cast onto clean gold substrates as described below. PMMA ($M_n = 28\,750$, $M_w/M_n = 1.03$) and PS ($M_n = 30\,300$, $M_w/M_n = 1.02$) were separately dissolved in THF with the concentrations of 0.14 mg/mL, and then these two solutions were mixed in different proportions. The mixtures were cast onto the same type of gold substrates used for polymer brush formation. The gold substrates were treated with the ozone cleaner before coating with ~1 μm thick film. The substrates were dried under air at room temperature for 4 h before the RAIR spectra were taken.

X-ray Photoelectron Spectroscopy. The substrates were analyzed immediately following immersion in the various solvents. XPS measurements were conducted using a Kratos Axis Ultra X-ray photoelectron spectrometer. Analysis was carried out under ultrahigh-vacuum conditions (10^{-9} Torr) using monochromatic Al Kα (1486.6 eV) excitation. The hemispherical energy analyzer was operated in the hybrid mode (a combined magnetic and electrostatic lens mode) with a 300 μm × 700 μm slot selected area aperture. The sample stage was grounded to the spectrometer, and the neutralizer was off in an effort to minimize sample damage. Spectra were collected in the constant pass energy (fixed analyzer transmission) mode. Survey spectra were collected using a pass energy of 160 eV with a scan step size of 1 eV. High-resolution spectra were collected with a pass energy of 20 eV and a scan step size of 0.1 eV. Angle-resolved XPS measurements were made at takeoff angles of 15°, 30°, and 90° relative to the sample surface.

Molecular Weight Determinations. The molecular weights of PS and PMMA were measured in toluene with a Waters Alliance 2690 separation module fitted with a Waters 2410 differential refractive index detector and a column heater set to 35 °C. Two 7.5 × 300 mm PLgel 5 μm MIXED-C columns from Polymer Laboratories were used and calibrated with PS and PMMA standards, respectively. The M_n and R_g were also measured with a MiniDAWN multi angle light scattering (MALS) detector from Wyatt Technologies.

Grafting Density Calculations (D_s). The grafting density in chains per surface area (D_s, chains/nm^2) may be calculated according to eq 1 from the molecular weight (M_n, g/mol), the thickness (Th, nm), density (d, g/nm^3), and Avogadro's number (N_a, molecules/mol), assuming a density of 1.047×10^{-21} g/nm^3 for bulk PS and 1.18×10^{-21} g/nm^3 for bulk PMMA.

$$D_s = \frac{ThdN_a}{M_n} \tag{1}$$

Solvent Immersion Experiments. The PS/PMMA mixed brushes were immersed in cyclohexane (50 °C) and hot isobutanol (100 °C) for 10 and 2 min, respectively. The substrates were then removed from the solvent and blown dry with nitrogen gas. These substrates will switch at room temperature; however, we have not yet examined their response under ambient conditions. The substrates were also found to be stable for short immersion times in hot solvents. For instance, after three cycles in hot cyclohexane (3 × 10 min) followed by THF, the contact angle remained the same, and we measured a slight change in thickness from 158 to 156 ± 1 nm. While we did not measure the thickness after three cycles in hot isobutanol (3 × 2 min), the contact angle and the intensity of the IR bands remained the same. We did not examine the effect of longer immersion times.

Atomic Force Microscopy. Two different instruments were used for these studies: First, the topographic images were acquired in contact mode on a TopoMetrix (Explorer model) scanning probe microscope with a silicon nitride tip. Second, the force−distance profiles were acquired on an Autoprobe CP Research AFM (formerly made by Park Scientific). The images were taken in contact mode using the large area 100 μm scanner. The tip was on a premounted chip carrier distributed by Park Scientific: model # ULCT-AUMT AB. The B cantilever was selected. The contact force was 50−60 nN. The machine was operated in constant force mode where deflection of the cantilever is used as input to a feedback circuit that moves the scanner up and down in Z responding to topography by keeping the cantilever deflection constant. A force vs distance curve is a plot of the deflection of the cantilever vs the extension of the piezoelectric scanner measured using a position-sensitive photodetector.

Results

Synthesis of the Mixed Brush. The polymer brushes were synthesized by immersing a SAM-coated substrate into a solution of monomer followed by UV irradiation. The SAM consists of a Au-thiolate AIBN type initiator (Figure 2), which has been described previously.[45] Our strategy for synthesizing a mixed brush from a single initiator is illustrated in Figure 3. Since AIBN is a fairly inefficient initiating system, owing to low absorptivity and a long half-life, we can irradiate for a specified period of time and be assured that active initiator will remain on the substrate. In our case we synthesized a PS brush first and then immersed the substrate back into a solution of toluene/MMA and continued irradiation. The net result after cleaning is a binary brush where the PS and PMMA are intercalated between each other (Figure 3c). This same strategy has been used for the thermal polymerization of mixed brushes.[21,25,32]

The SAMs of initiator **1** were adsorbed to gold-coated silicon wafers according to standard procedures. We then confirmed the SAM formation by static water contact angle (θ), RAIRS, and ellipsometry prior to polymerization. The substrate is then placed into a Schlenk tube with neat styrene and degassed prior to irradiation for 6 h at room temperature. The substrate is then removed and cleaned by Soxhlet extraction for

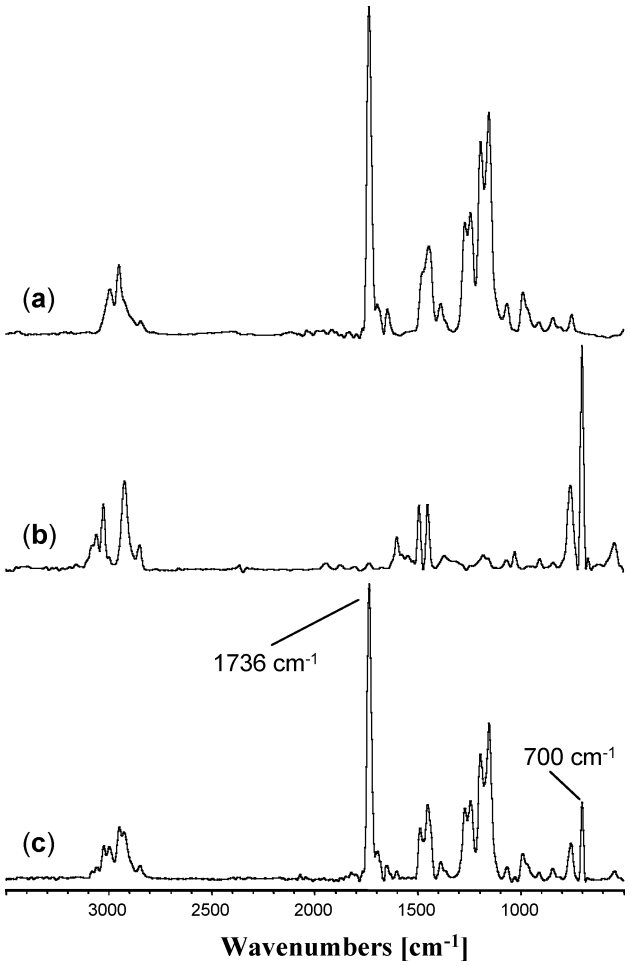

Figure 4. Reflection−absorption infrared spectra of (a) poly(methyl methacrylate) (PMMA) brush, (b) polystyrene (PS) brush, and (c) mixed brush of PMMA and PS.

10 h to yield a 70 ± 0.4 nm PS brush. This procedure was then repeated with a 50 wt % solution of MMA/toluene in lieu of styrene for a specified irradiation time. The substrates were then removed and cleaned by a second Soxhlet extraction. Control experiments with cast films of PS and PMMA demonstrate that these polymers are easily removed from the gold substrates by simply rinsing with THF. The presence of polymer after Soxhlet extraction strongly suggests that the polymer is tethered to the gold substrates. Furthermore, our previous work demonstrated that removal of physisorbed polymer from tethered polymer is complete after 10 h.[45]

The brush synthesis was confirmed by RAIRS, contact angles, and XPS. Figure 4a illustrates the RAIR spectrum of a PMMA brush with an intense carbonyl band around 1736 cm^{-1}. In contrast, the PS brush has no carbonyl; instead, it has aromatic C−H bands above 3000 cm^{-1} and around 700 cm^{-1} (Figure 4b). The mixed brush in Figure 4c has characteristic peaks for both PS and PMMA. Furthermore, θ for the substrate went from 64 ± 1° for the SAM to 88 ± 1° for the PS brush and ∼65 ± 1° for the mixed brushes; the θ for a neat PMMA brush is ∼61 ± 1°. In addition, the XPS spectrum of the PS brush is identical to cast films of PS, and the XPS of the mixed brush shows an intense O 1s peak that is consistent with the addition of PMMA. These results are also consistent with the mixed PS/PMMA brushes reported by Zhao.[41]

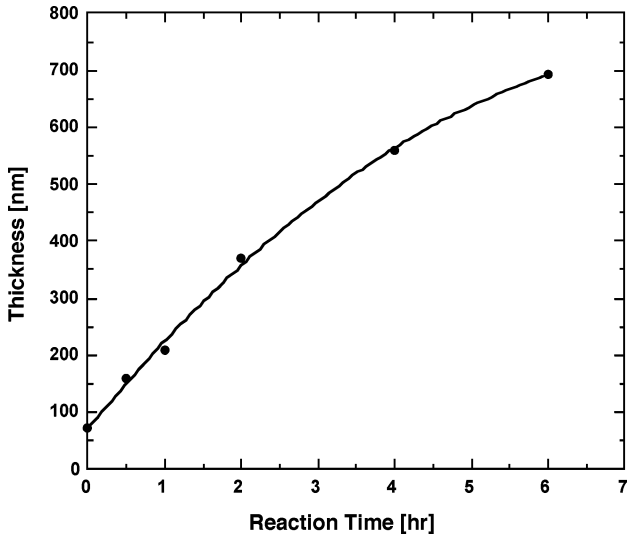

Figure 5. Film thickness vs reaction time for a mixed brush of polystyrene (PS) and poly(methyl methacrylate) (PMMA); at time zero we started with a 70 nm PS brush, which was immersed into a solution of methyl methacrylate and toluene.

The rate of film growth for the PMMA brush is much faster than that of PS as illustrated in Figure 5. The film thickness for the mixed brush doubles to ∼150 ± 1 nm after only 30 min, whereas it took 6 h to grow the 70 nm PS brush. This is not surprising since it is well-known that the rate of polymerization for MMA is much faster than styrene. Furthermore, the rate of PMMA growth for this mixed brush is slower than a single-component brush of PMMA. For example, the mixed brush exhibits a thickness of ∼200 ± 5 nm at 1 h compared to 226 ± 3 nm for the neat PMMA brush. At 2 h the mixed brush is ∼370 ± 5 nm compared to 735 ± 2 nm for the neat brush. We followed the growth of the mixed brush up to 6 h where the thickness reached ∼700 nm, which compared to ∼1245 nm for the neat PMMA brush. (It should be noted that the error in the optical thickness measurements may be large as the thickness approaches a micron.) The slower growth rate for the mixed brush is probably due to two factors: First, the concentration of active initiator is less for the mixed brush as it has already been irradiated for 6 h in styrene. Second, the diffusion of monomer to the surface may be slower due to increased crowding of polymer chains in the mixed brush compared to the neat PMMA brush.

Composition of the Mixed Brush. The composition of the mixed brush may be confirmed by a variety of techniques. For instance, the Cassie equation[46] (eq 2) can be used to estimate the mole ratios of each polymer from the water contact angle.

$$\cos(\theta) = \chi_1 \cos(\theta_1) + \chi_2 \cos(\theta_2) \qquad (2)$$

Here the observed contact angle (θ) for the mixed brush is related to the contact angle θ_1 and θ_2 of the single-component brushes and the fraction of each polymer at the surface χ_1 and χ_2; in this case θ_1 and θ_2 are 61° and 88° for neat PMMA and PS, respectively. Therefore, the surface composition is easily estimated by measuring the equilibrium contact angles of the neat polymers and the mixed brush. We expect that as the irradiation time increases for MMA, that the % PMMA in the brush should also increase. This is indeed what we observe as the static water contact angle goes from 65° after 30

min irradiation to 61° after 4 h. According to the Cassie equation, the % PMMA at the surface is 88% and 100% for 0.5 and 4 h irradiation times, respectively.

Since the Cassie equation does not take into account the surface morphology and roughness, which may have a large effect on the water contact angle, we sought alternative methods to determine the composition of the mixed brushes. In particular, XPS may be used to estimate the polymer composition by measuring the oxygen/carbon ratio. On the basis of the elemental composition of the two monomers, we derived eq 3 to calculate the ratio of oxygen to carbon in the mixed brush

$$\frac{C_o}{C_c} = \frac{2X_{PMMA}}{8 - 3X_{PMMA}} \tag{3}$$

where C_o and C_c are the atomic concentration of oxygen and carbon, and X_{PMMA} is the mole fraction of PMMA in the brush. If the film is 100% PMMA, then the C_o/C_c ratio should be 2/5 since there are two oxygen atoms and five carbons in the monomer, whereas there are eight carbons in styrene. Thus, after 30 min irradiation and at a 15° takeoff angle, the C_o and C_c at the surface are 19.6% and 80.4%, respectively, which correlates to 71% PMMA. The oxygen concentration increases at 4 h to yield a % PMMA of 84%. Both the Cassie equation and the XPS confirm the increase in PMMA over time.

Both water contact angles and XPS data yield estimates of the polymer composition. However, these are surface techniques that do not necessarily give an accurate measure of the % PMMA in the bulk film (i.e., below the first few nanometers). Therefore, we sought an alternative experimental technique that would yield an accurate measure of the polymer composition in the entire film. In principle, RAIR spectroscopy could be used to measure the absorbance of the PS and PMMA. To a first approximation, the absorbance of a particular vibration band (A_x) is proportional to the concentration of that functional group (c_x) in the polymer film. Equation 4 is derived from Beer's law

$$\frac{A_x}{A_y} = k\frac{c_x}{c_y} \tag{4}$$

where k is a proportionality constant that takes into account the difference in extinction coefficients between the two components. Thus, it should be possible to choose absorption bands that are unique to PMMA and PS. By measuring the ratio of the intensities of these bands, we should then be able to calculate the ratio of PMMA to PS in the entire film and not just at the air interface. This information is critical if one is to understand the switching dynamics of the films.

Figure 6 illustrates a method for determining the composition of a mixed polymer brush. First, the RAIR spectrum is used to identify absorption bands that are unique to the individual components. In our case PMMA has a carbonyl band at 1734 cm^{-1} (A_x), and PS exhibits an aryl-H bending mode at 701 cm^{-1} (A_y). The ratio of A_x/A_y absorptions should yield a good estimate of the mole fraction of PMMA and PS within the mixed brush. To test this strategy, we used a series of standard solutions of PS and PMMA and cast them onto gold. After obtaining the RAIR spectra, we plotted the absorption ratio vs PMMA concentration. This yields a calibration curve, which may then be used to determine

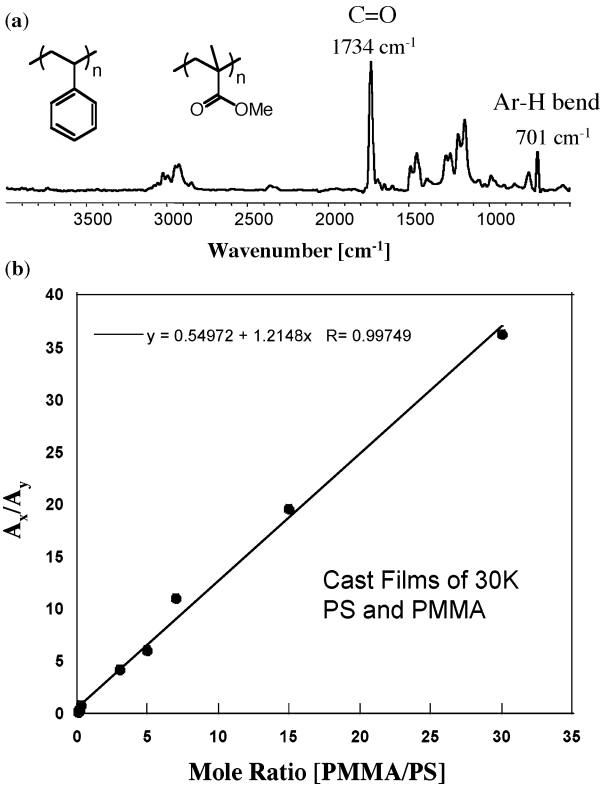

Figure 6. (a) Reflection−absorption infrared spectrum can be used to find absorption bands that are unique to each polymer in the mixed brush. (b) The molar concentration of poly(methyl methacrylate) (PMMA) in the mixed brush can be derived from eq 4 and a calibration curve from a series of mixtures with known concentration. In this case we chose the carbonyl band (1734 cm^{-1}) for PMMA as A_x and an Ar−H bending mode at 701 cm^{-1} for polystyrene (PS) as A_y.

the mole ratio of PMMA by simply calculating the ratio of the absorption maximum for the carbonyl and Ar−H bands in the mixed brush.

The concentration of PMMA in the mixed brush was calculated for various reaction times. As described in Figure 7, the % PMMA increases rapidly, and after 30 min of irradiation, the film is nearly 50% PMMA. After 1 h the % PMMA increases to 70% and is greater than 90% after 6 h. Since the RAIRS technique is sensitive to orientational effects, in this case transition dipoles parallel to the surface do not absorb, we sought an independent technique to verify these results. Therefore, we used XPS at a 90° takeoff angle to calculate the % PMMA as described previously. Surprisingly, the XPS results match perfectly with the RAIRS (Figure 7), suggesting that the surface concentration is a good indicator of the bulk when the substrate is pretreated with a solvent where both polymers are soluble, in this case THF. At least with these samples it appears that both polymers come to the surface in the same proportions as is present in the bulk film, which is below the XPS detection limit (∼6−8 nm for a 90° takeoff angle).[47] Therefore, both XPS and RAIRS can be used to estimate the bulk composition of mixed brushes.

These AIBN-type initiators form two active radicals, only one of which is bound to the surface; therefore, polymer is always formed in the bulk solution. For our SAMs only one thiol is bound to the surface; therefore, the anchored initiating radical will be similar to the radical released into the bulk solution. The terminal thiol does not appear to significantly alter the number-

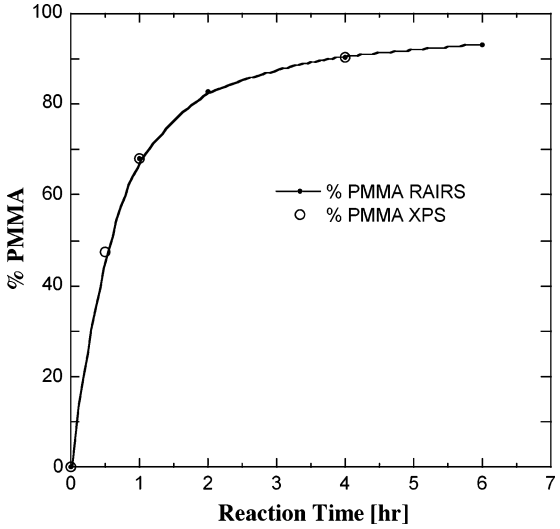

Figure 7. Percent poly(methyl methacrylate) (% PMMA) in the film increases over time, and both reflection−absorption infrared spectroscopy (RAIRS) and X-ray photoelectron spectroscopy (XPS) can be used to independently verify the composition of the mixed brush. The XPS measurements were taken at 90° takeoff angle.

Table 1. Number-Average Molecular Weight (M_n) of Poly(methyl methacrylate) Recovered from the Bulk Solution[a]

rxn time [h]	M_n [Da]	M_w/M_n	DP
0.5	515 100	1.46	5145
1	404 800	1.54	4043
2	400 500	1.47	4000
6	320 400	1.45	3200

[a] The polystyrene brush had M_n = 56 610, M_w/M_n = 1.49, and DP = 543; DP = degree of polymerization. All data were acquired by GPC/MALS.

average molecular weight (M_n) by chain transfer, and it has been shown previously that the M_n and polydispersity (PDI = M_w/M_n) of the polymer recovered from the bulk solution are similar to those of the grafted polymer.[18] We monitored the M_n vs reaction time for PMMA and found a similar trend as with PS, namely, that the M_n decreases slightly over time and the PDI is consistent with a typical free radical polymerization under these conditions (Table 1);[48] control experiments with clean gold substrates yield similar PDI. Furthermore, the M_n of the PS from the bulk was 56 100 Da, which is almost an order of magnitude less than for PMMA. Thus, the kinetic chain length, or degree of polymerization (DP), for the PMMA chains in the 50/50−PS/PMMA brush is 5145, compared to 543 for the PS. It is also likely that the number of grafted PMMA chains is much less than that of PS since the initiation rate should be similar for both polymerizations, and the PS substrates were irradiated for 7 h compared to 30 min for the PMMA polymerizations. This further supports a longer kinetic chain length for grafted PMMA relative to PS.

Switching of the Mixed Brush. We have found that mixed brushes of PS and PMMA are conveniently switched by immersion in cyclohexane and isobutanol; others have used acetone,[33] chloroform, and acetic acid to switch PS/PMMA brushes.[41] As Figure 8 illustrates, immersion in cyclohexane brings the PS to the liquid interface and causes the PMMA to collapse into the interior of the film. The reverse occurs when the substrate is treated with a polar solvent such as isobutanol. Furthermore, treatment with THF brings both polymers to the liquid/air interface. The switching occurs in a matter of minutes with hot solvent and is slower at room temperature.

The switching behavior of these binary brushes was examined with water contact angles, XPS, and RAIRS. As Table 2 illustrates, after a 30 min irradiation in MMA, followed by a Soxhlet extraction in THF, the bulk composition is nearly 48% PMMA by RAIRS. In addition, according to eq 2, the static water contact angle of 66° correlates to 80% PMMA at the air interface. Furthermore, we used variable angle XPS to graze the surface with a 15° takeoff angle and to probe more deeply with a 90° takeoff angle. The air/liquid interface is enriched in PMMA with a PMMA composition of 71% at 15°, compared to 53% at 90°; the larger takeoff angle yields results that are more indicative of the bulk composition.

After immersion into cyclohexane for 10 min at 50 °C, we anticipated that the PS would come to the surface because the nonpolar solvent disfavors the more polar PMMA. Indeed, θ increases to 84° as the % PMMA at the surface plummets to 17% by eq 2 (θ for neat PS is 88°). The displacement of PMMA is even more dramatic as evidenced by the XPS data where the PMMA composition at 15° dropped from 71% to 4% after treatment in cyclohexane (Figure 9e). The % PMMA at a 90° takeoff angle increased to 10% (Figure 9b). Thus, the amount of PMMA at the surface decreases dramatically and increases as we probe deeper into the film; there is almost a complete absence of oxygen at the air/liquid interface. Furthermore, the switching is completely reversible over several cycles and remains so after several months.

We also examined the switching behavior after treatment in isobutanol for 2 min at 100 °C. The water contact angle decreased from 65° to 61°, indicating an increase in the PMMA concentration, in this case from 85% to 100% according to eq 2. Interestingly, at a 15° takeoff angle, the PMMA concentration (by eq 3) did not change and remained at 71% (Figure 9f), while at 90° the PMMA increased to 75% from 53% (Figure 9c). This suggests a more heterogeneous interface after isobutanol treatment compared to the cyclohexane treatment. Furthermore, the % PMMA near the surface increased slightly from THF. The small change in θ also suggests that the air/liquid interface is dominated by PMMA since θ is much closer to neat PMMA (61°) than to PS (88°).

The morphology of these substrates was examined by AFM after each solvent treatment. As illustrated in Figure 10a, the 50% PMMA film shows some evidence of nanophase separation after immersion in THF. At this point, both PS and PMMA are present at the surface, as confirmed by XPS, and the root-mean-square (rms) roughness is ±3.6 nm. There appears to be some indentations that are randomly dispersed throughout the surface. Upon immersion into cyclohexane, the morphology changes (Figure 10b) and exhibits more phase separation with a slight decrease in rms roughness to ±2.5 nm. In addition, the substrate appears to have peaks rather than indentations. When this film is immersed directly into isobutanol, the morphology changes again, as described in Figure 10c. Interestingly, the peaks are sharper and much higher than in the previous instance, and the roughness increases significantly to ±5.9 nm. Furthermore, upon immersion back

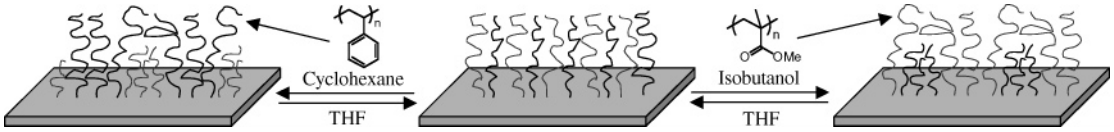

Figure 8. Switching of a polystyrene/poly(methyl methacrylate) (PS/PMMA) mixed brush by treatment with various solvents. A nonpolar solvent like cyclohexane yields a surface enriched in PS, whereas treatment with a polar solvent like isobutanol yields a surface enriched in PMMA. Treatment with tetrahydrofuran (THF) brings both polymers to the surface.

Table 2. Switching Parameters for Binary Brushes as a Function of Reaction Time in Methyl Methacrylate from a 70 nm Polystyrene Brush

polymerization time (h)	% PMMA in mixed brush	solvent	static contact angle (deg)	% PMMA calcd from XPS		
				from θ	15°	90°
0.5	47.5	THF	66	80	71	53
		cyclohexane	84	17	4	10
		THF	65	84		
		cyclohexane	86	8		
		THF	65	85		
		cyclohexane	84	14		
		THF	65	84	71	53
		isobutanol	60	100	71	75
		THF	66	83		
		isobutanol	61	100		
		THF	65	85		
		isobutanol	61	97		
1	68	THF	62	96	80	88
		cyclohexane	80	32	33	64
		THF	61	98	80	88
		isobutanol	60	100	82	89
4	90	THF	61	100	85	92
		cyclohexane	61	98	83	90
		THF	60	100		
		isobutanol	60	100	84	93
6	93	THF	61	100		92
		cyclohexane	62	95		86
		THF	61	100		
		isobutanol	60	100		89

[a] The percentage of poly(methyl methacrylate) (% PMMA) in the bulk film (left) is calculated from reflection absorption infrared spectroscopy, and the surface composition (right) is determined by static water contact angles (θ) and variable-angle X-ray photoelectron spectroscopy (XPS). The water contact angles were measured consecutively after immersion in tetrahydrofuran (THF), cyclohexane, or isobutanol.

into THF (Figure 10d), the substrate returns to a similar morphology as before, with indentations and a slightly smoother surface (±2.4 nm). It should be noted that these micrographs were not over the exact same area; however, they are representative of the entire surface.

The morphology of the mixed brushes was also compared to that of neat PS and PMMA films with similar thicknesses. In particular, both the neat PS (Figure 10e) and PMMA (Figure 10f) substrates are very smooth with an rms roughness of approximately ±2 nm for both. The morphology of the two differ in that PMMA exhibits very sharp peaks, while the domains in the PS substrate are more blurred and rather broad. Importantly, the neat PS substrate is more similar to the mixed brush after treatment in cyclohexane than either THF or isobutanol. This is consistent with the PS coming to the air interface and displacement of the PMMA. The same is true for PMMA after treatment in isobutanol, where PMMA dominates the air interface and both exhibit well-defined peaks compared to PS.

The solvent treatments have some effect on the roughness and the average height of the various domains as summarized in Table 3. In particular, the average height and roughness are always larger for the mixed brushes than for the single-component brushes. The largest values are after treatment in isobutanol. Interestingly, the morphology for a 90% PMMA brush is quite responsive after the solvent treatments even though the water contact angle is not. The rms roughness and average height for the 10/90 PS/PMMA mixed brush after treatment in THF were ~3 and 11 nm, respectively. These values do not change after immersion in cyclohexane; however, they more than double after immersion in isobutanol.

Tsukruk has used AFM to examine the mechanical properties of brush films.[49] For example, it is possible to generate a force−distance curve as shown in Figure 11; the tip is pressed into the film, and then it is allowed to spring back. The slope of the advancing line can yield information about the stiffness or elasticity of the substrate. In this case the 50/50 PS/PMMA brush is quite stiff with a slope of 0.91 and lies between that of neat PS (0.83) and PMMA (0.98) brushes of similar thickness.

Discussion

Synthesis of the Mixed Brush. There are a variety of methods that have been used to synthesize mixed brushes. In particular, GT strategies have been successfully employed for grafting to SAM substrates and bare silicon. For instance, annealing of hydroxyl- and carboxylate-terminated polymers has been used to graft polymer onto bare silicon wafers.[37,50] Typically a thin film is cast onto silicon, and the film is annealed above the T_g for 24−48 h, resulting in films with very low grafting densities and ~5 nm in thickness. Alternatively, one may cast a polymer film such as poly(glycidyl methacrylate) and graft it to silicon by annealing at high temperature. Since this polymer has additional reactive groups, epoxides in this case, additional polymers may be cast and annealed onto the PGMA layer.[23] Furthermore, Minko has cast films of poly(tetrafluoroethylene) (PTFE) onto silicon and subsequently oxidized the PTFE, so that polymers could be grafted by annealing.[34] Yet another GT technique has utilized glycidyl-terminated SAMs,[24,26,28] which presumably yields thicker films and higher grafting densities than simple annealing on native silicon oxide. Finally, Frank and others have used benzophenone-terminated SAMs to photochemically excite and subsequently abstract hydrogen atoms from cast polymer films.[29,51] Thus, some of the polymer is grafted to the SAM, and the remaining physisorbed polymer is rinsed away.

Since GT methods yield low grafting densities and films less than 10 nm in thickness, alternative GF approaches have been developed. For instance, Luzinov has grafted PGMA to silicon by annealing and then chemically treating the polymer so that ATRP could be used for a subsequent grafting step from the modified PGMA.[27] Others have used SAM-based initiators rather than polymer substrates for GF. In particular, Brittain used reverse atom transfer radical polymerization (RATRP) to graft block copolymers to AIBN-type initiators on silicon.[38] Furthermore, Zhao utilized a mixed

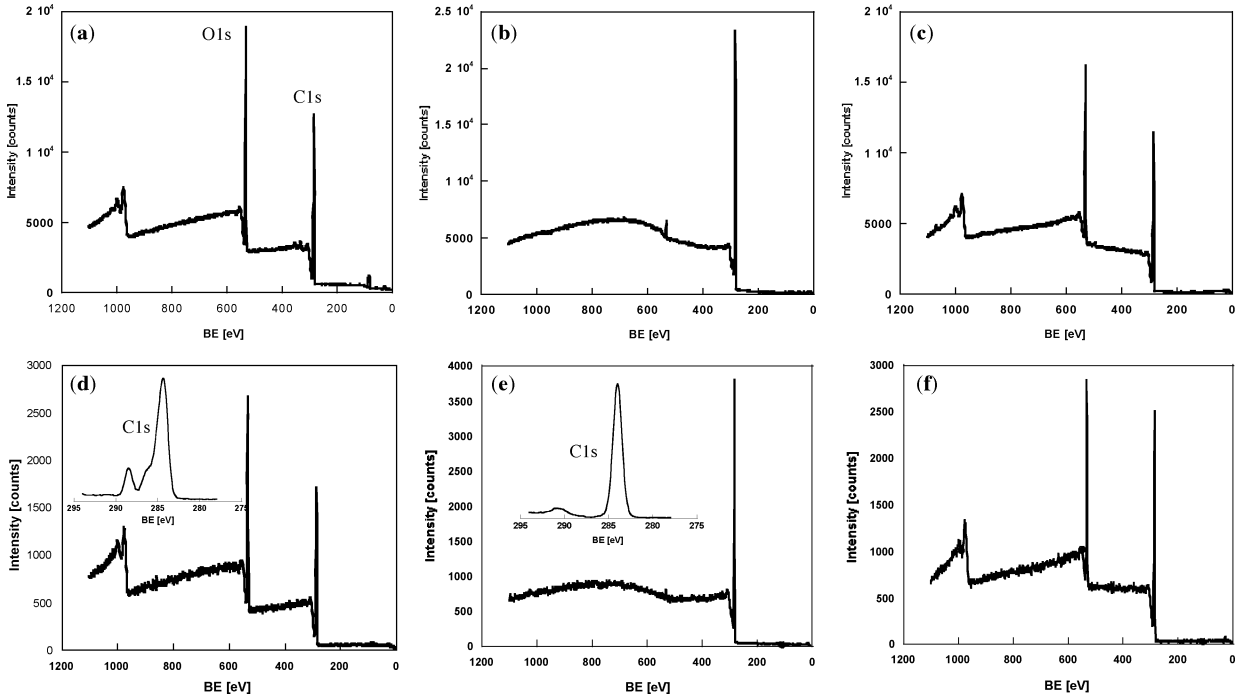

Figure 9. X-ray photoelectron spectra of a 50/50 polystyrene/poly(methyl methacrylate) mixed brush after immersion in various solvents: (a) tetrahydrofuran at 90° takeoff angle; (b) cyclohexane at 90° takeoff angle; (c) isobutanol at 90° takeoff angle; (d) tetrahydrofuran at 15° takeoff angle; (e) cyclohexane at 15° takeoff angle; (f) isobutanol at 15° takeoff angle. The C 1s region is expanded in (d) and (e).

monolayer approach with a combination of ATRP and nitroxide-mediated radical initiators that were activated at different temperatures.[42]

The mixed monolayer approach is attractive since it is possible to immobilize two or more initiators that may be activated independently. After the first polymer is grafted, the film may be cleaned and reactivated under different conditions in order to synthesize a binary or even ternary brush. However, there are three major complications in this approach that should be considered: First, it is nontrivial to quantify the proportions of each initiator within the SAM. One cannot simply assume that the solution concentrations during deposition will be represented in the SAM, since the adsorption kinetics for the individual components may be quite different depending on their respective structures. This is particularly problematic for alkylthiolates on gold; therefore, it is desirable to utilize RAIRS and XPS to try to quantify the structure of the SAM prior to polymerization. The concentration of initiator at the surface will play some role in the grafting density and the response parameters of the resulting polymer film. Second, phase separation may inhibit the grafting of the second polymer when the two are incompatible. This may result in an uneven distribution of the two polymers within the film. To minimize this, care should be taken to ensure that the polymerization conditions utilize a nonselective solvent (i.e., a solvent where both polymers are soluble). Finally, the initiation efficiency of the two different systems could be problematic if they differ significantly. For instance, if one initiator exhibits slow kinetics, there will be fewer grafted chains relative to the faster initiator under similar reaction conditions. Therefore, longer reaction times may be required to achieve similar grafting densities for the two brushes.

Because of the complications with mixed SAMs, single-component SAMs have been utilized for the synthesis of mixed brushes. In particular, Zhao used a Y-shaped chlorosilane initiator for deposition onto silicon.[41] Each branch at the air interface contained a different initiator, in this case ATRP, and nitroxide-mediated initiators were used. This helps to alleviate the problems associated the difference in adsorption kinetics for mixed SAMs. In addition, the incompatible polymers are forced together since both will be grafted to the same precursor. Alternatively, others have taken advantage of the inherent inefficiency of AIBN to synthesize mixed brushes from single-component SAMs, as described in Figure 3.[21,25,32] One advantage to AIBN is that both thermal and photoinitiation are possible.

The mixed brushes of PS/PMMA that we synthesized differ from those described previously in several respects. First, the GF technique yields much higher grafting densities than is available via GT methods. Second, the photoinitiation strategy is more rapid than thermal initiation. Third, our films are significantly thicker than those synthesized by Zhao and Brittain via controlled radical polymerizations from SAMs. Fourth, previous PS/PMMA brushes were tethered to silicon substrates via alkylsilanes, whereas we used alkylthiolates on gold. We do not anticipate that the underlying substrate or SAM will play a significant role in the composition or switching dynamics of mixed brushes, provided the SAMs are densely packed and the initiating moieties are identical. Finally, alkylthiolate SAMs are less stable at temperatures above 60 °C[52] but are quite stable at room temperature.

Composition of the Mixed Brush. If we are to develop meaningful structure−property relationships, then it is critically important to quantify the fraction of each homopolymer within these mixed brushes. This is not trivial for ultrathin films since techniques such as XPS and contact angles only describe the first few nanometers at the air/liquid interface. Furthermore, RAIRS is very sensitive to orientational effects within

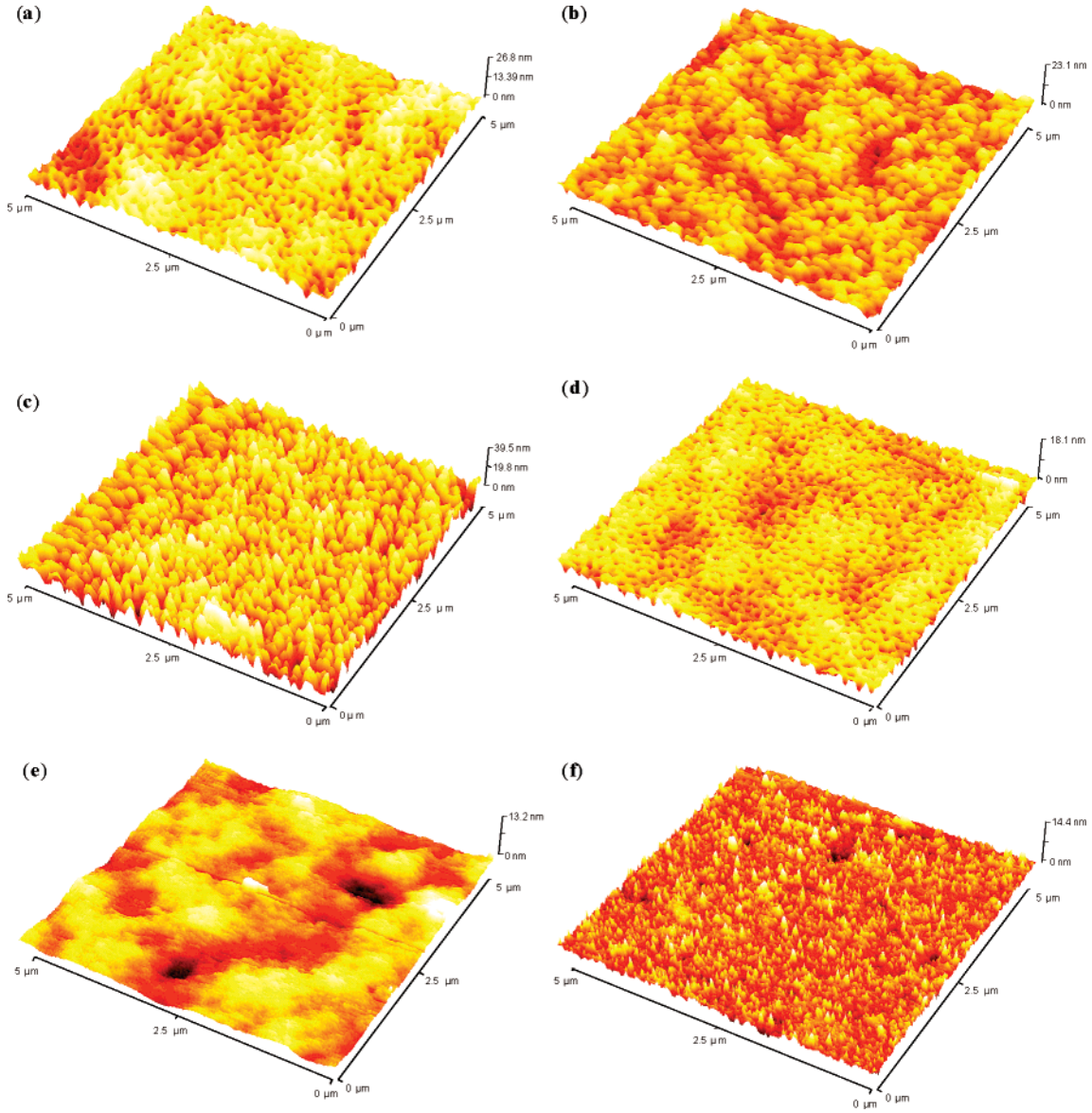

Figure 10. Atomic force microscopy (AFM) micrographs of a polystyrene/poly(methyl methacrylate) (PS/PMMA) brush after sequential immersions in (a) tetrahydrofuran (THF), (b) cyclohexane, (c) isobutanol, and (d) THF. Micrographs (e) and (f) represent neat PS and PMMA brushes, respectively, after treatment in THF.

Table 3. Surface Roughness for Polymer Substrates after Sequential Immersion in Various Solvents, Measured by Atomic Force Microscopy[a]

substrate					
% PS	% PMMA	solvent	film thickness (nm)[b]	rms roughness (± nm)	av domain height (nm)
100	0	THF	165	2.1	7.8
0	100	THF	205	1.9	6.5
50	50	THF	150	3.6	16.0
50	50	cyclohexane		2.5	11.6
50	50	isobutanol		5.9	22.9
50	50	THF		2.4	11.1
10	90	THF	559	2.8	11.1
10	90	cyclohexane		3.1	9.8
10	90	isobutanol		6.9	23.2

[a] rms = root mean square; THF = tetrahydrofuran; PS = polystyrene; PMMA = poly(methyl methacrylate). [b] Measured by ellipsometry.

the film due to the polarization of the light, which favors transition dipoles normal to the substrate. Thus, the intensities of the various absorption bands may change due to environmental perturbations, even though the bulk composition of the brush is constant. Nevertheless, we demonstrate here that these techniques can be used in concert to yield a good estimate of both the polymer composition in the bulk film and at the air/liquid interface.

The static water contact angle for a 50/50 PS/PMMA brush is 66° after treatment in THF, which is much closer to neat PMMA than to neat PS (Table 2). This suggests that the air/liquid interface is dominated by PMMA; the Cassie equation provided a rough estimate of 80% PMMA at the surface. In addition, from XPS we calculated 71% PMMA at a 15° takeoff angle compared to 53% at a 90° takeoff angle. Therefore, the concentration of PMMA is greater at the surface than within the bulk. This is also consistent with the M_n data (Table 1), which suggests that the grafted PMMA chains are much longer than the PS chains. In this case the DP for PMMA is more than 9 times that of PS. The grafting density for PMMA is also likely to be much less than that of PS since the PS brush was irradiated for 7 h vs only 30 min for PMMA; presumably, the rate of initiation is similar, as the irradiation intensity was identical.

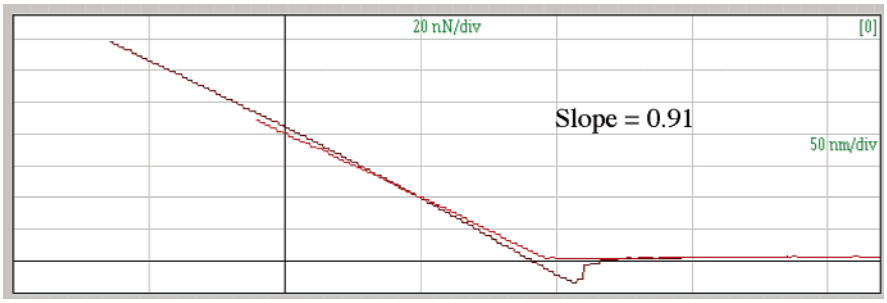

Figure 11. Force−distance curve from an atomic force microscopy experiment for a 50/50 polystyrene/poly(methyl methacrylate) (PS/PMMA) mixed brush. The slope of the advancing line may be used to estimate the elasticity or stiffness of the substrate. In this case the slope lies between that of neat PS and PMMA brush films; a slope of 1 implies a very hard surface.

We propose that the PMMA chains are sticking out well beyond the PS layer and are folding back onto the PS, thus enriching the first few nanometers at the air/liquid interface with PMMA. As Figure 7 illustrates, the RAIRS data are a nearly perfect match with the XPS at 90° takeoff angle. Thus, we have a high degree of confidence in the bulk concentration of PMMA within the films. Assuming that the PMMA concentration at the surface is best represented by the XPS data at a 15° takeoff angle, then the Cassie equation predicts a water contact angle of 70° with a 71% PMMA composition. This is in close agreement with the observed contact angle of 66° vs a predicted contact angle of 75° if the air/liquid interface were a 50/50 mixture. Therefore, the evidence strongly suggests that the first few nanometers of these films are dominated by PMMA after treatment with THF.

Switching of the Mixed Brush. One of our goals is to understand and control the response of mixed brushes to environmental perturbations. The effect of solvent polarity and hydrophobicity is an obvious place to start since the substrates may be readily characterized after immersion into various solvents. For these studies we chose THF as our nonselective solvent; cyclohexane and isobutanol were chosen as selective solvents for PS and PMMA, respectively.

As the data in Table 2 illustrates, these films are quite responsive to solvent treatments. In particular, immersion in cyclohexane results in a θ of 84° for the 50/50 PS/PMMA substrate. Furthermore, XPS confirms that PS dominates the air/liquid interface with concentrations of 96% and 90% at 15° and 90° takeoff angles, respectively. Upon immersion into isobutanol, θ decreases dramatically and is consistent with neat PMMA. Interestingly, the XPS shows nearly 30% PS at a 15° takeoff angle; this compares to only 4% PMMA after immersion in cyclohexane. This suggests that the PMMA is able to rearrange so that it penetrates below the PS surface. It is possible that PS is less responsive; however, the larger amount of PS at the surface after isobutanol treatment could be a result of the much higher grafting density of PS relative to PMMA in the film. As the reaction time increases, the density of PMMA increases and the films become less responsive and are dominated by PMMA. Finally, immersion in THF brings the system back to equilibrium and demonstrates the reversibility of the switching.

It is interesting to compare our results with those of Zhao, who used a Y-shaped initiator so that PMMA and PS were tethered to the same SAM precursor molecule.[41] In Zhao's approach the PMMA and PS chains are forced together, whereas in our approach the first polymer brush (PS) may force the PMMA to phase-separate into localized regions where the PS concentration is low. Therefore, it is possible that the PMMA is not randomly distributed within the PS, but rather localized PMMA-rich domains are randomly distributed between localized PS domains. However, we do not believe this is the case since the PMMA polymerization was performed in toluene, which is a good solvent for both PMMA and PS in this range of M_n's. Furthermore, the grafting density of PS is relatively high, which would inhibit the formation of localized regions of PMMA with a high grafting density during the deposition of the second brush.

Zhao described a mixed brush where the M_n's for PS and PMMA were 14 and 17.5 kDa, respectively. Thus, both chains are about the same length, and they should be equally distributed within the substrate. In this case, the advancing water contact angle (θ_a) increased from 83° after immersion in chloroform to 91° after immersion into cyclohexane, which is selective for PS. Furthermore, the % PMMA by XPS decreased from 43% to 26% from chloroform to cyclohexane. This change is much less than what we observed for our brush system (53% to 10% at 90° takeoff angle) and suggests that the chains tethered to Y-shaped SAMs are less mobile. Zhao also examined a similar brush by immersion from chloroform into acetic acid. In this case the θ_a increased from 91° to 100° for a mixed brush where the M_n for both PS and PMMA was ~27 000 Da. Furthermore, the XPS data indicated an increase in the PMMA concentration from 22% to 50% after immersion in acetic acid. Interestingly, the contact angle is significantly larger than neat PS, and much larger than our 50/50 brush, which was 61° after immersion in isobutanol. This indicates a higher concentration of PS at the air/liquid interface for the Y-shaped brushes even though the bulk concentration is about 50/50 (assumed from M_n data).

However, comparisons between our binary brush and Zhao's Y-shaped brush are complicated by significant differences in the structure and composition of the brushes. First, Zhao reported a thickness around 28 nm, compared to ~160 nm for our 50/50 brush. We also calculated grafting densities D_s (chains/nm^2) for these two systems. In our 50/50 PS/PMMA brush, the PS was deposited first, and we calculated D_s of 0.78 (chains/nm^2). To estimate the D_s of the mixed brush, it is necessary to estimate the grafting density for PMMA. The D_s for a neat PMMA brush after 1 h of irradiation was calculated at 0.40 for a 226 nm film. The D_s should be approximately half this at 30 min or 0.20; however, it is likely that the additional PS would reduce the overall D_s relative to a neat PMMA brush. In principle, a neat PS brush would have a D_s of 1.67, compared to 0.20 for PMMA in a 150 nm film; by taking the average

of these two limits, we estimate that the D_s for the mixed brush is 0.94 chains/nm^2. Thus, the PMMA increases the grafting density by an additional 0.16 chains/nm^2. In comparison, Zhao first deposited a PMMA layer that resulted in a D_s of 0.60 chains/nm^2 for a 17.5 kDa PMMA brush. The second polymerization of PS would presumably double the surface density to 1.20 chains/nm^2 and resulted in a 14 kDa/17.5 kDa PS/PMMA brush. In both cases the films possess fairly high D_s, where our films are less dense by approximately 25%. It is possible that the increased D_s for the Y-shaped brush is responsible for the lack of response relative to our mixed brush. Another difference lies in the fact that we used THF instead of chloroform for the nonselective solvent. Although we have not examined chloroform, we find it unlikely that the two solvents will alter the results as PS and PMMA are very soluble in both solvents. Also, future efforts should compare these systems in both isobutanol and acetic acid.

Brittain and co-workers have studied diblock copolymer brushes of PS and PMMA, and these results were fairly consistent with our mixed brushes. For instance, they showed that the θ_a went from 73° after immersion in dichloromethane to 92° after immersion in methylcyclohexane. The tethered block copolymer films were quite thin (~30 nm) and exhibited reversible switching. As with Zhao's work, the brushes were tethered to silicon via siloxane-based SAMs, whereas our work is with gold and a thiolate-based SAM. While the quality of the underlying SAM does play an important role in the overall polymerization and composition of the final film, we do not believe that the underlying SAM is playing a dominant factor in the response similarity and differences between these systems; rather, M_n and D_s are more important and are likely to dominate regardless of the underlying SAM. Unfortunately, Brittain did not report the M_n of the diblock so we were not able to calculate D_s. However, the PMMA layer was only $^1/_4$ as thick as the underlying PS layer. Nevertheless, the films responded quite well to the solvent treatments, as evidenced by $\theta_a \sim 75°$ after treatment in dichloromethane. This indicates that the positioning of the PMMA is as important as the bulk concentration.

Russell and co-workers carried out another interesting study where they grafted random copolymers of PS and PMMA to silicon substrates. These were low-density brushes synthesized by a GT strategy, and the M_n of the polymers was kept constant as the % PMMA was altered. They observed that θ_a increased smoothly from 69° for neat PMMA to 90° for neat PS. The 50/50 copolymer exhibited a θ_a of 82°, roughly halfway between the two limits. Interestingly, the Cassie equation fails to predict the composition of these random copolymer substrates. For instance, eq 2 predicts a % PMMA of 86% for the substrate that is known to exhibit a 50% PMMA composition. This is similar to our results where eq 2 predicted 80% PMMA for a substrate that was shown by RAIRS and XPS to have a 50/50 composition. Thus, the Cassie equation should only be used for a qualitative comparison between substrates of similar structure.

We have used XPS as a quantitative tool for determining the % PMMA in these films even though it is known that PMMA films are damaged from the intense X-ray beams used in these experiments. In fact, Russell has suggested that XPS should not be used for this purpose. However, our results and those of Zhao indicate that XPS can be accurate under some conditions. In particular, Zhao reported a thickness of 28.3 nm and an oxygen concentration of 11.25% for a 14 kDa/17.5 kDa PS/PMMA Y-shaped brush; we calculated a % PMMA of 43% (by eq 3), and he reported a θ_a of 82°. This contact angle is in good agreement with what Russell reported for a 50/50 grafted random copolymer brush film. Furthermore, the data in Figure 7 are compelling as the same composition is found for techniques that are completely independent of each other. We believe most of the damage occurring during XPS analysis, and described previously, is actually caused by electrons and thermal radiation coming from windowed nonmonochromatic X-ray sources. In addition, there is also damage caused by the photoelectrons, Auger electrons, and secondary electrons as well as energetic photons emitted from the sample. But by using a monochromatic source, and not using the neutralizer, one can eliminate the exposure of the sample to the unnecessary radiation, thus minimizing the damage. Nevertheless, care must be taken when measuring the percent composition by XPS, particularly with respect to the takeoff angle, which significantly affects the results in multicomponent brushes.

Ade and co-workers have studied grafted polymer blends of PS and PMMA, which were synthesized by annealing hydroxy-terminated homopolymer brushes of PS and PMMA.[37] These were mixed together and grafted to the surface to form low-density brushes. They reported a θ of 77° for a 50/50 PS/PMMA blend, which is in reasonable agreement with Zhao and Russell. The fact that our 50/50 brush has a θ of 65° suggests that in our system the PMMA is preferentially wetting the first few nanometers of the film, which is probably due to the much longer chain length for the PMMA relative to PS.

The morphology of our brushes changes after each solvent treatment as evidenced by AFM (Figure 10). In particular, the 50/50 brush after treatment in THF exhibits some nanophase separation and nanoindentations; the morphology appears different from what Minko and Stamm have termed a "ripple" phase for binary brushes of PPFS/PMMA in a nonselective solvent.[33] In this case, our AFM micrographs do not appear to form long cylindrical domains. However, after treatment in cyclohexane our 50/50 brush develops broader peaks, which become sharper and taller after immersion in isobutanol. These last two phases appear similar to what Minko and Stamm have referred to as a "dimple" phase. Interestingly, the morphology after immersion in isobutanol is also very similar to what has been described by Zhao for Y-shaped brushes after immersion in acetic acid. He also observed sharper domains and peaks when the PMMA came to the surface. It appears to be a general trend that as the PS concentration increases, the domains in the AFM micrographs become broader and more blurred. Furthermore, in both the Y-shaped brushes and those described here, the PMMA rich interfaces are always rougher than the PS-enriched interfaces.

The response of the 10/90 PS/PMMA brushes is also very interesting. While the contact angle of this substrate is insensitive to the solvent treatments, the morphology may change significantly. For instance, the rms roughness and the average peak height by AFM do not change significantly from THF to cyclohexane, as described in Table 3. However, upon immersion into

isobutanol, the rms roughness increases to ±6.9 nm from approximately ±3 nm in THF or cyclohexane, and the height increases from 11 nm in THF or cyclohexane to 23 nm in isobutanol. Thus, even though the substrate is dominated by PMMA at the air/liquid interface and within the bulk, the low concentration of underlying PS may be affecting the air/liquid interface. Of course, this could simply be an artifact of PMMA brushes and have little to do with the underlying PS. Indeed, Zhao has shown that neat PMMA brushes do undergo a significant rearrangement after immersion in acetic acid, which is selective for PMMA. Clearly more study is needed to probe the effect of the underlying brush.

Conclusions

We have synthesized binary brushes of PS and PMMA from an AIBN type free radical initiating SAM. The evidence suggests that the PMMA chains are much longer than the PS chains, which requires that the grafting density for PMMA is significantly lower than that of PS for the 50/50 brush. The composition of these brushes may be quantified by XPS and RAIRS and θ. Care should be taken in using the Cassie equation to describe the air/liquid interface, as large errors are likely depending on the system. Furthermore, XPS and RAIRS should be used in tandem to confirm the bulk composition as well as the air/liquid interface.

It is clear that the mixed brushes of PS and PMMA respond to various solvents, and this response is reversible. The θ values were fairly consistent with the literature, and the change in oxygen concentration with takeoff angle confirms the presence of layered phase separation. Furthermore, AFM shows a dimple phase with lateral segregation in cyclohexane and isobutanol and a third phase with less lateral segregation in THF. Treatment with THF brings both PS and PMMA to the air/liquid interface, whereas treatment in cyclohexane and isobutanol brings PS and PMMA to the air/liquid interface, respectively. The roughest films result from PMMA after immersion in isobutanol. These films exhibit both lateral and perpendicular nanophase separation in the selective solvents, and the air/liquid interface is dominated by PMMA after treatment in a nonselective solvent.

Future efforts should be directed at examining the switching process in much greater detail by altering the immersion times and solvent polarities. Detailed comparisons should be made between the four basic mixed brush systems; these include block copolymers, Y-shaped SAMs, mixed SAMs, and randomly distributed brushes from a single SAM. In addition, we plan on examining the effects of grafting density, film thickness, and M_n on the response characteristics of brush films.

Acknowledgment. We thank Dr. Ling Zang, Dr. Xiaomei Yang, and Ms. Dee Gates for help with the AFM images and measurements. Funding was provided by the Materials Technology Center at SIUC and the National Science Foundation under Grant CHE-0094195. The XPS measurements were carried out in the Center for Microanalysis of Materials, University of Illinois, which is partially supported by the U.S. Department of Energy under Grant DEFG02-91-ER45439 and the University of Illinois. J.F. thanks SIUC for a doctoral fellowship.

References and Notes

(1) (a) Rühe, J.; Knoll, W. *J. Macromol. Sci., Polym. Rev.* **2002**, *C42*, 91−138. (b) Zhao, B.; Brittain, W. J. *Prog. Polym. Sci.* **2000**, *25*, 677−710. (c) Nagasaki, Y.; Kataoka, K. *Trends Polym. Sci.* **1996**, *4*, 59−64. (d) Milner, S. T. *Science* **1991**, *251*, 905−914.

(2) (a) Rouhi, A. M. *Chem. Eng. News* **1999**, *77*, 51−59. (b) Perry, C. In *Chemistry of Advanced Materials: An Overview*; Interrante, L. V., Hampden-Smith, M. J., Eds.; Wiley-VCH: Weinhem, 1998; pp 499−563.

(3) Niklason, L. E.; Gao, J.; Abbott, W. M.; Hirschi, K. K.; Houser, S.; Marini, R.; Langer, R. *Science* **1999**, *284*, 489−493.

(4) Rimmer, S. In *Emerging Themes in Polymer Science*; Ryan, A. J., Ed.; Royal Society of Chemistry: Cambridge, 2001; pp 89−99.

(5) (a) James, C. D.; Davis, R.; Meyer, M.; Turner, A.; Turner, S.; Withers, G.; Kam, L.; Banker, G.; Craighead, H.; Isaacson, M.; Turner, J.; Shain, W. *IEEE Trans. Biomed. Eng.* **2000**, *47*, 17−21. (b) Langer, R. *Acc. Chem. Res.* **2000**, *33*, 94−101. (c) Cameron, N. R. In *Emerging Themes in Polymer Science*; Ryan, A. J., Ed.; Royal Society of Chemistry: Cambridge, 2001; p 100. (d) Santini, J. T.; Richards, A. C.; Scheidt, R.; Cima, M. J.; Langer, R. *Angew. Chem., Int. Ed.* **2000**, *39*, 2396−2407. (e) Klugherz, B. D.; Jones, P. L.; Cui, X.; Chen, W.; Meneveau, N. F.; DeFelice, S.; Connolly, J.; Wilensky, R. L.; Levy, R. J. *Nat. Biotechnol.* **2000**, *18*, 1181−1184.

(6) (a) Ishang-Riley, S. L.; Okun, L. E.; Prado, G.; Applegate, M. A.; Ratcliffe, A. *Biomaterials* **1999**, *20*, 2245−2256. (b) Tidwell, C. D.; Ertel, S. I.; Ratner, B. D.; Tarasevich, B. J.; Atre, S.; Allara, D. L. *Langmuir* **1997**, *13*, 3404−3413. (c) Ratner, B. D.; Johnston, A. B.; Lenk, T. J. *J. Biomed. Mater. Res.: App. Biomater.* **1987**, *21*, 59−90.

(7) Black, F. E.; Hartshorne, M.; Davies, M. C.; Roberts, C. J.; Tendler, S. J. B.; Williams, P. M.; Shakesheff, K. M. *Langmuir* **1999**, *15*, 3157−3161.

(8) Lenz, P. *Adv. Mater.* **1999**, *11*, 1531−1534.

(9) Kataoka, D. E.; Trolan, S. M. *Nature (London)* **1999**, *402*, 794−797.

(10) Xia, Y.; Qin, D.; Yin, Y. *Curr. Opin. Colloid Interface Sci.* **2001**, *6*, 54−64.

(11) Kricka, L. *Clin. Chim. Acta* **2001**, *307*, 219−223.

(12) Krishnan, M.; Namasivayam, V.; Lin, R.; Pal, R.; Burns, M. A. *Curr. Opin. Biotech.* **2001**, *12*, 92−98.

(13) Lahiri, J.; Isaacs, L.; Grzybowski, B.; Carbeck, J. D.; Whitesides, G. M. *Langmuir* **1999**, *15*, 7186−7198.

(14) Rouhi, A. M. *Chem. Eng. News* **1997**, *75*, 41−45.

(15) Sullivan, T. P.; Huck, W. T. S. *Eur. J. Org. Chem.* **2003**, 17−29.

(16) (a) Edmondson, S.; Osborne, V. L.; Huck, W. T. S. *Chem. Soc. Rev.* **2004**, *33*, 14−22. (b) Pyun, J.; Kowalewski, T.; Matyjaszewski, K. *Macromol. Rapid Commun.* **2003**, *24*, 1043−1059.

(17) Dyer, D. J. *Adv. Funct. Mater.* **2003**, *13*, 667−670.

(18) Dyer, D. J.; Feng, J.; Fivelson, C.; Paul, R.; Schmidt, R.; Zhao, T. In *Polymer Brushes*; Advincula, R. C., Brittain, W. J., Rühe, J., Caster, K., Eds.; Wiley-VCH: Weinheim, 2004; Chapter 7, pp 129−150.

(19) Prucker, O.; Konradi, R.; Schimmel, M.; Habicht, J.; Park, I.-J.; Rühe, J. In *Polymer Brushes*; Advincula, R. C., Brittain, W. J., Rühe, J., Caster, K., Eds.; Wiley-VCH: Weinheim, 2004; Chapter 23, pp 449−469.

(20) (a) Zhang, J.; Xu, X.; Chen, J.; Kang, E. *Thin Solid Films* **2002**, *413*, 76−84. (b) Zhang, J.; Cui, C. Q.; Lim, T. B.; Kang, E. *Macromol. Chem. Phys.* **2000**, *201*, 1653−1661.

(21) Sidorenko, A.; Minko, S.; Schenk-Meuser, K.; Duschner, H.; Stamm, M. *Langmuir* **1999**, *15*, 8349−8355.

(22) Hayashi, S.; Abe, T.; Higashi, N.; Niwa, M.; Kurihara, K. *Langmuir* **2002**, *18*, 3932−3944.

(23) Ionov, L.; Houbenov, N.; Sidorenko, A.; Minko, S.; Stamm, M. *Polym. Mater. Sci. Eng. Prepr.* **2004**, *90*, 104−105.

(24) Houbenov, N.; Minko, S.; Stamm, M. *Macromolecules* **2003**, *36*, 5897−5901.

(25) Minko, S.; Usov, D.; Goreshnik, E.; Stamm, M. *Macromol. Rapid Commun.* **2001**, *22*, 206−211.

(26) Minko, S.; Patil, S.; Datsyuk, V.; Simon, F.; Eichhorn, K.-J.; Motornov, M.; Usov, D.; Tokarev, I.; Stamm, M. *Langmuir* **2002**, *18*, 289−296.

(27) Luzinov, I.; Klep, V.; Minko, S.; Iyer, K. S.; Draper, J.; Zdyrko, B. *Polym. Mater. Sci. Eng. Prepr.* **2004**, *90*, 224−225.

(28) Ionov, L.; Minko, S.; Stamm, M.; Gohy, J.-F.; Jérôme, Scholl, A. *J. Am. Chem. Soc.* **2003**, *125*, 8302−8306.

(29) Hoffmann, F.; Wolff, T.; Minko, S.; Stamm, M. *Polym. Mater. Sci. Eng. Prepr.* **2004**, *90*, 374−375.

(30) (a) Lemieux, M.; Minko, S.; Usov, D.; Stamm, M.; Tsukruk, V. V. *Langmuir* **2003**, *19*, 6126−6134. (b) Lemieux, M. C.;

Minko, S.; Usov, D.; Shulha, H.; Stamm, M.; Tsukruk, V. V. *Polym. Mater. Sci. Eng. Prepr.* **2004**, *90*, 372−373.
(31) Lemieux, M. C.; Shulha, H.; Kovalev, A.; Minko, S.; Tsukruk, V. V. *Polym. Mater. Sci. Eng. Prepr.* **2004**, *90*, 207−208.
(32) Lemieux, M.; Usov, D.; Minko, S.; Stamm, M.; Shulha, H.; Tsukruk, V. V. *Macromolecules* **2003**, *36*, 7244−7255.
(33) Minko, S.; Müller, M.; Usov, D.; Scholl, A.; Froeck, C.; Stamm, M. *Phys. Rev. Lett.* **2002**, *88*, 035502−1.
(34) Minko, S.; Müller, M.; Motornov, M.; Nitschke, M.; Grundke, K.; Stamm, M. *J. Am. Chem. Soc.* **2003**, *125*, 3896−3900.
(35) de Gennes, P. G. *Macromolecules* **1980**, *13*, 1069−1075.
(36) (a) Marko, J. F.; Witten, T. A. *Phys. Rev. Lett.* **1991**, *66*, 1541−1544. (b) Marko, J. F.; Witten, T. A. *Macromolecules* **1992**, *25*, 296−307. (c) Lai, P.-Y *J. Chem. Phys.* **1994**, *100*, 3351−3357. (d) Soga, K. G.; Zuckermann, M. J.; Guo, H. *Macromolecules* **1996**, *29*, 1998−2005. (e) Zhulina, E.; Balazs, A. C. *Macromolecules* **1996**, *29*, 2667−2673. (f) Müller, M. *Phys. Rev. E* **2002**, *65*, 030802-1.
(37) Winesett, D. A.; Story, S.; Luning, J.; Ade, H. *Langmuir* **2003**, *19*, 8526−8535.
(38) Sedjo, R. A.; Mirous, B. K.; Brittain, W. J. *Macromolecules* **2000**, *33*, 1492−1493.
(39) Boyes, S. G.; Brittain, W. J.; Weng, X.; Cheng, S. Z. D. *Macromolecules* **2002**, *35*, 4960−4967.
(40) Mansky, P.; Liu, Y.; Huang, E.; Russell, T. P.; Hawker, C. *Science* **1997**, *275*, 1458−1460.
(41) Zhao, B.; Haasch, R. T.; MacLaren, S. *J. Am. Chem. Soc.* **2004**, *126*, 6124−6134.
(42) Zhao, B.; He, T. *Macromolecules* **2003**, *36*, 8599−8602.
(43) Zhao, B. *Polymer* **2003**, *44*, 4079−4083.
(44) Schmidt, R.; Zhao, T.; Green, J.-B.; Dyer, D. J. *Langmuir* **2002**, *18*, 1281−1287.
(45) Paul, R.; Schmidt, R.; Feng, J.; Dyer, D. J. *J. Polym. Sci., Part A: Polym. Chem.* **2002**, *40*, 3284−3291.
(46) (a) Cassie, A. B. D.; Baxter, S. *Trans. Faraday Soc.* **1944**, *40*, 546. (b) Cassie, A. B. D. *Discuss. Faraday Soc.* **1948**, *3*, 11−16. (c) Garbassi, F.; Morra, M.; Occhiello, E. In *Polymer Surfaces: From Physics to Technology*; Wiley-VCH: Weinheim, 1998; Chapter 4, p 169. (d) Israelachvili, J. N.; Gee, M. L. *Langmuir* **1989**, *5*, 288−289.
(47) Briggs, D. *Surface Analysis of Polymers by XPS and Static SIMS*; Cambridge University Press: Cambridge, UK, 1998; Chapter 2, p 39.
(48) (a) Prucker, O.; Rühe, J. *Macromolecules* **1998**, *31*, 602−613. (b) Ajayaghosh, A.; Francis, R. *J. Am. Chem. Soc.* **1999**, *121*, 6599−6606.
(49) Lemieux, M.; Minko, S.; Usov, D.; Stamm, M.; Tsukruk, V. V. *Langmuir* **2003**, *19*, 6126−6134.
(50) Wang, J.; Kara, S.; Long, T. E.; Ward, T. C. *J. Polym. Sci., Part A: Polym. Chem.* **2000**, *38*, 3742−3750.
(51) Prucker, O.; Naumann, C. A.; Rühe, J.; Knoll, W.; Frank, C. W. *J. Am. Chem. Soc.* **1999**, *121*, 8766−8770.
(52) (a) Bhatia, R.; Garrison, B. J. *Langmuir* **1997**, *13*, 765−769. (b) Clegg, R. S.; Reed, S. M.; Hutchison, J. E. *J. Am. Chem. Soc.* **1998**, *120*, 2486-2487. (c) Sandhyarani, N.; Pradeep, T. *Vacuum* **1998**, *49*, 279−284. (d) Schönherr, H.; Ringsdorf, H.; Jaschke, M.; Butt, H.-J.; Bamberg, E.; Allinson, H.; Evans, S. D. *Langmuir* **1996**, *12*, 3898−3904.

MA048681W